Dynamically Tunable Multifunction Attenuator Based on Graphene Integrated Dual-Mode Microstrip Resonators

Zhi-Qiang Yang , Quan-Long Wen , Chi Fan , Bian Wu * , Yang Qiu

Posted Date: 20 December 2024

doi: 10.20944/preprints202412.1760.v1

Keywords: multifunction attenuator; dynamically tunable; graphene sandwiched structure; microstrip dual-mode resonators

Article

Dynamically Tunable Multifunction Attenuator Based on Graphene Integrated Dual-Mode Microstrip Resonators

Zhi-Qiang Yang [1,†], Quan-Long Wen [2,†], Chi Fan [2], Bian Wu [2,*] and Yang Qiu [3,]

[1] Key Laboratory of Advanced Science and Technology on High Power Microwave, Northwest Institute of Nuclear Technology, Xi'an, China
[2] National Key Laboratory of Antennas and Microwave Technology, Xidian University, Xi'an 710071, China
[3] School of Mechano-Electronic Engineering, Xidian University, Xi'an 710071, China
* Correspondence: bwu@mail.xidian.edu.cn
† These authors contributed equally to this work.

Abstract: In this paper, a design method of tunable multifunctional attenuators is proposed by analyzing the characterization of dual-mode microstrip resonators loaded by graphene sandwiched structure (GSS). Firstly, the odd-even mode method is applied to analyze the resonance characteristics of two common GSS loaded dual-mode resonators, which clearly describe the influence of graphene on these resonators. Then, two kinds of multifunction attenuator with dynamically tunable attenuation are proposed based on graphene integrated dual-mode resonators, which enables controllable characteristics and multi-frequency transmission options for traditional attenuating devices. Finally, all the proposed multifunctional attenuators are fabricated and measured. The experimental results are in good agreement with the simulation results, which further verifies the conclusions and design method proposed in this paper.

Keywords: multifunction attenuator; dynamically tunable; graphene sandwiched structure; microstrip dual-mode resonators

1. Introduction

With the continuous development and of preparation methods and processing technology, graphene-based materials are being widely used in the design of new electromagnetic devices due to their excellent properties [1]-[5]. In the microwave band, graphene-based materials prepared by different improved processes often have different properties, thus suitable for the design of different devices. For example, the properties of omnidirectional resistance and easy printing of graphene ink is particularly suitable for the design of absorbers with periodic structure [6]-[8] and multi-way dividers [9]. Multilayer graphene films through high temperature annealing and rolling and with the properties of high conductivity and flexibility are ideal for the design of pressure sensors [10] and wearable antennas [11]. In addition to the above materials, graphene-based materials with controllable electrical conductivity is the hotspot recently. Both of few-layer graphene flakes and graphene nanoplates have controllable conductivity and small size, which make them suitable for the design of tunable attenuator [12]-[15] and reconfigurable antenna [16]. However, tunable devices based on graphene nanoplates always require additional bias circuits, which make it difficult to be apply to the design of multifunctional devices. Graphene sandwiched structure (GSS) is a kind of graphene-based material processed from two monolayers graphene and ionic liquid, which also has controllable conductivity and can be used for the design of tunable attenuator [17]-[19]. The surface resistance of GSS can be controlled only by applying a vertical voltage on the two pieces of monolayer graphene. So, GSS is well suited for the design of integrated devices. For example, by loading GSS on spoof surface plasmon polariton (SSPP) transmission line with a low noise amplifier (LNA) chip, a

 doi:10.20944/preprints202412.1760.v1

dynamically tunable integrated device for attenuation, amplification and transmission can be designed [18]. Since no additional bias circuit is required, the loading of the GSS does not affect the operation of the LNA.

In this paper, the GSS is integrated with two kinds of microwave dual-mode resonators to analyze the influence of graphene on the different modes of these resonators. Then, two conclusions and a design method for multifunction attenuator are proposed through comparing the resonant intensity of different modes. At last, some multifunction attenuators are designed and fabricated according to the proposed method. The measured results show that all these multifunction attenuators can achieve controllable attenuation by applying vertical voltage on the GSS be loaded on the resonators.

2. Characterization of Dual-Mode Microstrip Resonators Loaded with Graphene Sandwiched Structure

The microstrip dual-mode resonators have open structure and clear electromagnetic field distribution, making them easier to be integrated with graphene. In order to study the effect of loading graphene on the dual-mode resonators, GSSs are loaded on the different positions of two common resonators.

The geometry of the GSS loaded open-ended resonator with centrally loaded open stub resonator is exhibited in Figure 1a. GSS is loaded on position 1 (GSS is loaded on the open-ended resonator) or position 2 (GSS is loaded on the open stub) to influence the resonant characteristics of this resonator. When GSS is loaded on position 1, d represents the distance between GSS and the center of the open-ended resonator. When GSS is loaded on position 2, d1 represents the distance between GSS and the beginning of the open stub. Lg and Wg are the length and width of GSS. All the parameters are given in Table 1. Figure 1b depicts the equivalent circuit of GSS loaded open-ended resonator with centrally loaded open stub dual-mode resonators, which can be analyzed by odd-even mode method. Figure 1c shows the disassembling diagram of Figure 1b, when GSS loaded on position 1 or position 2 respectively. Then, the influence of loading GSS on the dual-mode resonator can be theoretically analyzed by calculating the input admittance of the odd-even mode resonant structure. When GSS is loaded on position 1, the input admittance of odd-mode and even-mode can be calculated by the formula (1)-(3) and (4)-(6), respectively.

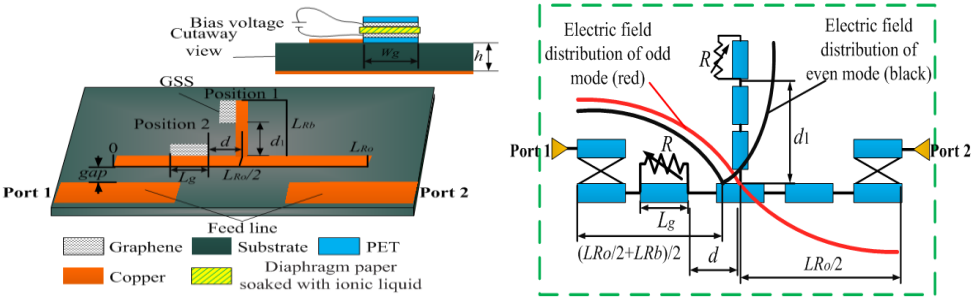

(a) (b)

Preprints.org (www.preprints.org) | NOT PEER-REVIEWED | Posted: 20 December 2024 doi:10.20944/preprints202412.1760.v1

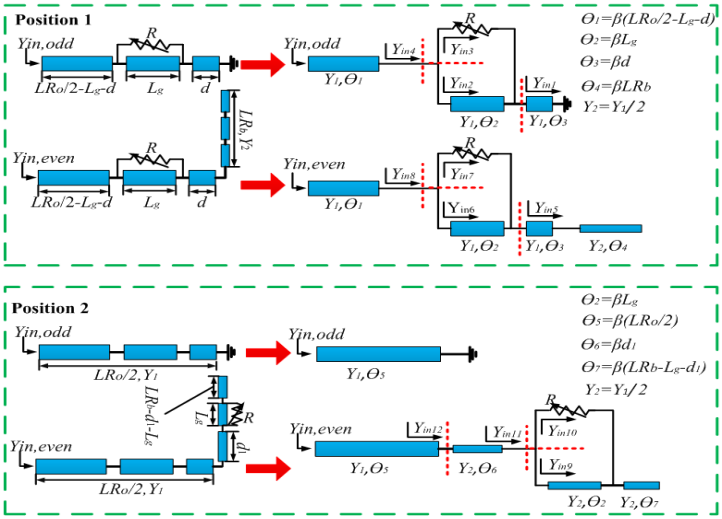

(c)

Figure 1. (a) Configuration;(b) The equivalent circuit;(c) The detail sketch of odd-even mode of the GSS loaded open-ended resonator with centrally loaded open stub.

Table 1. Design Parameters of Gss Loaded Open-Ended Resonator with Centrally Loaded Open Stub.

Parameter	Value	Parameter	Value
L_{Ro}	40mm	gap	0.5mm
L_{Rb}	5mm	ε_r	2.65
L_g	5mm	h	1mm
W_g	1mm		

$$Y_{in,\mathrm{odd}} = Y_1 \frac{Y_{in4} + jY_1 \tan\theta_1}{Y_1 + jY_{in4} \tan\theta_1} \quad (1)$$

$$Y_{in4} = Y_{in2} + Y_{in3} = Y_1 \frac{Y_{in1} + jY_1 \tan\theta_2}{Y_1 + jY_{in1} \tan\theta_2} + \frac{RY_1Y_{in1} + 1}{Y_{in1}} \quad (2)$$

$$Y_{in1} = -jY_1 / \tan\theta_3 \quad (3)$$

$$Y_{in,\mathrm{even}} = Y_1 \frac{Y_{in8} + jY_1 \tan\theta_1}{Y_1 + jY_{in8} \tan\theta_1} \quad (4)$$

$$Y_{in8} = Y_{in6} + Y_{in7} = \frac{RY_1Y_{in5} + 1}{Y_{in5}} + Y_1 \frac{Y_{in5} + jY_1 \tan\theta_2}{Y_1 + jY_{in5} \tan\theta_2} \quad (5)$$

$$Y_{in5} = jY_1 \frac{Y_1 \tan\theta_3 + Y_2 \tan\theta_4}{Y_1 - Y_2 \tan\theta_3 \, \mathrm{an}\, \theta_4} \quad (6)$$

According to the formula (1)-(6), the surface resistance of GSS has no effect on the imaginary part of input admittance but has a great influence on the real part. Similarly, the same method can be used to calculate the odd-even mode input admittance when GSS loaded on position 2. The calculation results are given in formula (7)-(10) and the same conclusion can be drawing. The full wave simulation results of GSS loaded open-ended resonator with centrally loaded open stub are shown in Figure 2, which cannot only verify the calculation results, but also summarize the influence of loading graphene on the dual-mode resonator.

As can be seen from the Figure 2, when GSS is loaded on position 1 and d=5mm, graphene can attenuate the resonance intensity of odd-mode but have little influence on even-mode. When GSS is loaded on position 1 and d=15mm, graphene can attenuate the resonance intensity of both odd-mode and even-mode. when GSS is loaded on position 2 and d1=0mm, graphene can attenuate the resonance intensity of even-mode but have no influence on odd-mode. Moreover, when graphene can effectively attenuate the resonant mode, the smaller the surface resistance of GSS, the bigger the attenuation amplitude. So, wo can draw conclusions that the effect of graphene on the resonator is

 doi:10.20944/preprints202412.1760.v1

related to the electric field distribution of the resonant mode and for GSS loaded open-ended resonator with centrally loaded open stub, the resonance intensity of both two modes can be controlled independently and flexibly by changing the loading position and surface resistance of GSS.

$$Y_{in,\mathrm{odd}} = -jY_1/\tan\theta_5 \quad (7)$$

$$Y_{in,\mathrm{even}} = Y_1 \frac{Y_{in12} + jY_1 \tan\theta_5}{Y_1 + jY_{in12} \tan\theta_5} \quad (8)$$

$$Y_{in12} = Y_2 \frac{Y_{in11} + jY_2 \tan\theta_6}{Y_2 + jY_{in11} \tan\theta_6} \quad (9)$$

$$Y_{in11} = \frac{jY_2 \tan\theta_7}{jRY_2^{\,2} \tan\theta_7 + 1} + jY_2 \frac{Y_2 \tan\theta_2 + Y_2 \tan\theta_7}{Y_2 - Y_2 \tan\theta_2 \,\mathrm{an}\,\theta_7} \quad (10)$$

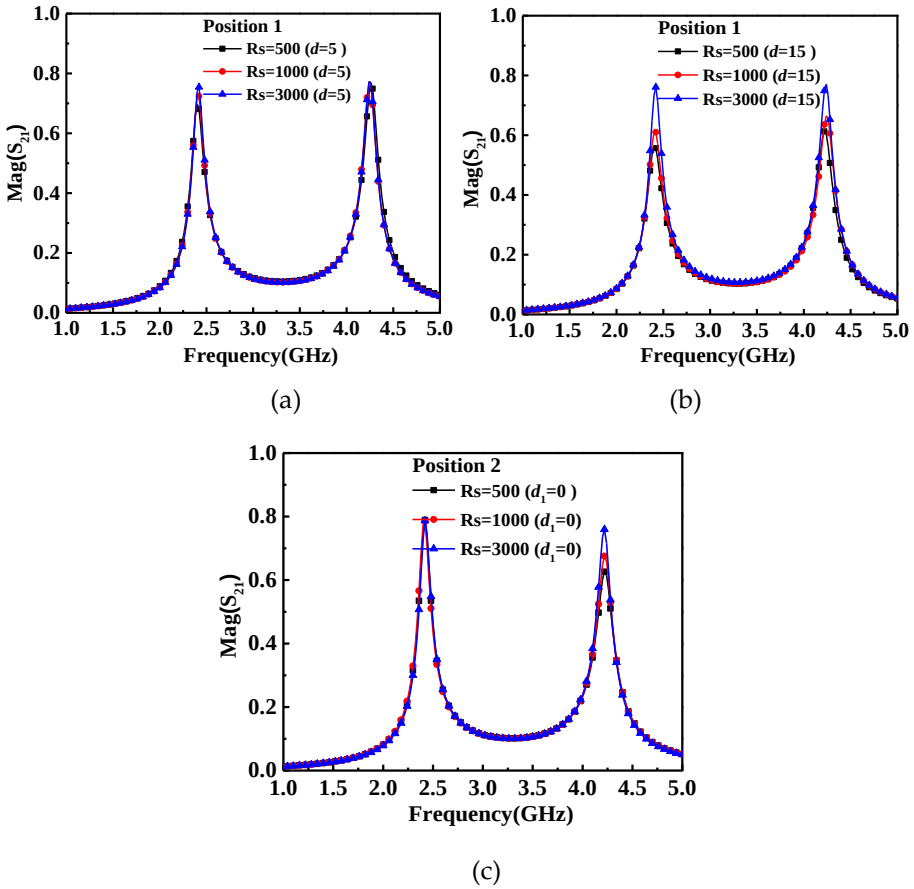

Figure 2. The relation between Rs and transmission coefficient of GSS loaded open-ended resonator with centrally loaded open stub (a) position1, d=5;(b) position1, d=5; (c) position2, d1=0.

3. Tunable Multifunctional Attenuator Based on Graphene Integrated Dual-Mode Microstrip Resonators

According to conclusion from section 2, controllable dual-band filtering attenuators can be designed. This section will design two dual-band tunable filtering attenuator with similar performance but using different design principle. Figure 3 shows two dual-band filtering attenuators based on GSS loaded open-ended resonator with centrally loaded open stub and all the parameters are given in Table 2. Tunable dual-band filtering attenuator I is composed of two open-ended resonators with centrally loaded open stub of different size. The larger one forms the first passband and the higher passband is formed by the smaller one. GSS 1can attenuate the odd and even modes of the large resonator, so the surface resistance of GSS1 can control the attenuation of the first passband. Similarly, the attenuation of the second passband can be controlled by controlling the surface resistance of GSS 2.

Preprints.org (www.preprints.org) | NOT PEER-REVIEWED | Posted: 20 December 2024 doi:10.20944/preprints202412.1760.v1

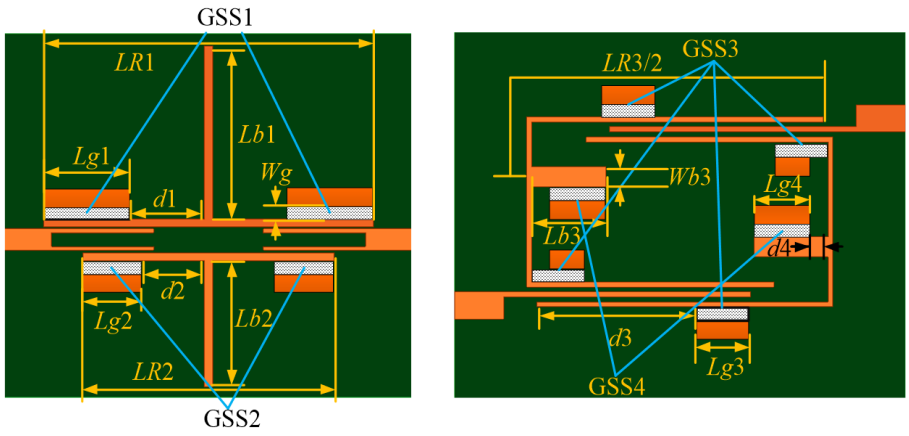

(a) (b)

Figure 3. (a)Tunable dual-band filtering attenuator I. (b) Tunable dual-band filtering attenuator II.

Tunable dual-band filtering attenuator II is composed of two identical open-ended resonators with centrally loaded open stub and the work principle is different form dual-band filtering attenuator I. The first passband of filtering attenuator II is composed of two odd modes of two identical resonators and the second passband is composed of two even modes of the resonators. Therefore, GSS3 loaded on the open resonators can control the attenuation of the first passband and GSS4 loaded on the open stubs can control the attenuation of the second passband.

Table 2. The Dimensions of The Filtering Attenuator.

Parameter	Value	Parameter	Value
Lr2	25.9mm	Ws	9.3mm
Lg2	13mm	D	8.6mm
Ls	8.4mm	ε_r	2.2
Wr2	1mm	h2	0.787mm
Wg2	0.95mm		

Figure 4 depicts the simulation results of tunable dual-band filtering attenuators I and II. For attenuators I, controlling the surface resistance of GSS1 can achieve controllable attenuation of 1.5-7.1dB at the first passband while keeping the second passband unchanged. Controlling the surface resistance of GSS3 loaded on attenuators II can achieve controllable attenuation of 1.3-6.7dB in the first passband while keeping the second passband unchanged. The second passband of these two dual-band filtering attenuators can also be tuned independently by controlling the surface resistance of GSS2 and GSS4. When GSS1 and 2 loaded on attenuator I and GSS3 and 4 loaded on attenuator II change simultaneously, the two passbands of these two attenuators can be tuned at the same time.

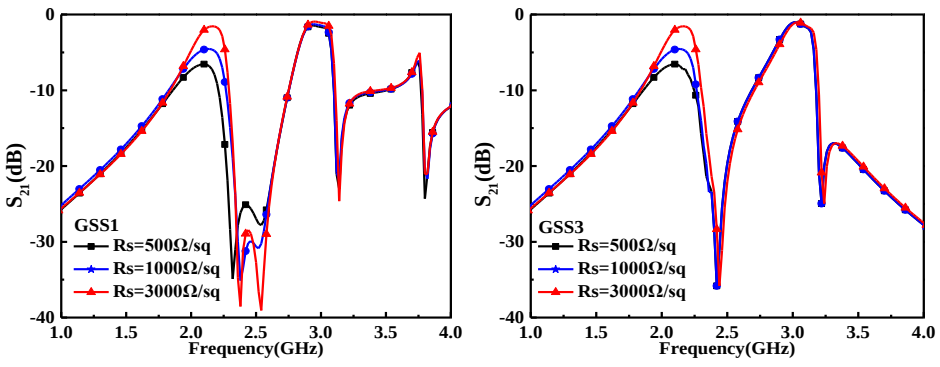

(a) (b)

Preprints.org (www.preprints.org) | NOT PEER-REVIEWED | Posted: 20 December 2024 doi:10.20944/preprints202412.1760.v1

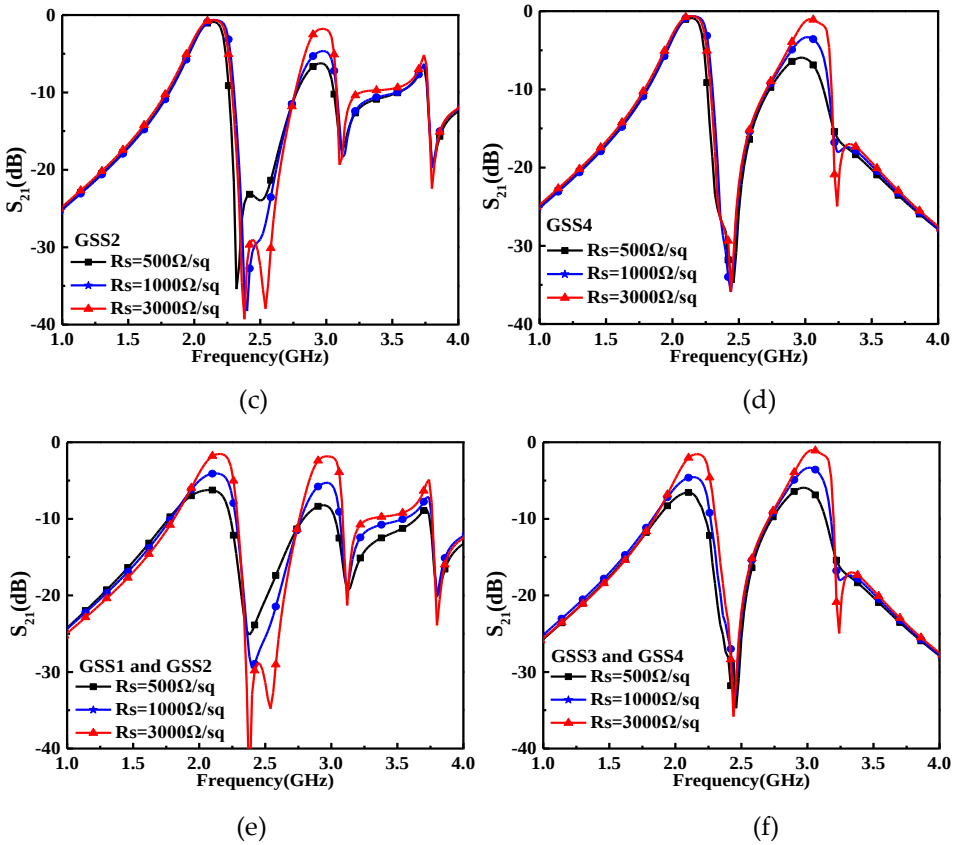

Figure 4. The simulation results of tunable dual-band filtering attenuators I and II. (a)control the surface resistance of GSS1 (b)control the surface resistance of GSS3 (c)control the surface resistance of GSS2 (d)control the surface resistance of GSS4 (e)control the surface resistance of GSS1and 2 (f)control the surface resistance of GSS3 and 4.

In order to verify the design of tunable dual-band filtering attenuators, two prototypes are fabricated and measured. The whole circuit is implemented on F4B substrate with a dielectric constant of 2.2 and a thickness of 1mm, as shown in Figure 5a,b. Meanwhile, the measured results of these attenuators are shown in Figure 5c,d. According to the results, by applying a bias voltage of 0-5V to the GSSs loaded on these attenuators, two dual-band filtering attenuators can achieve 1.7-7.9dB,1.6-7.2 dB and 1.8-7.5 dB,1.3-6.9 dB attenuation in their two passbands. The measured results achieve good attenuation control, which can not only verify the design principle but also demonstrate the characteristics of GSS loaded open-ended resonator with centrally open stub.

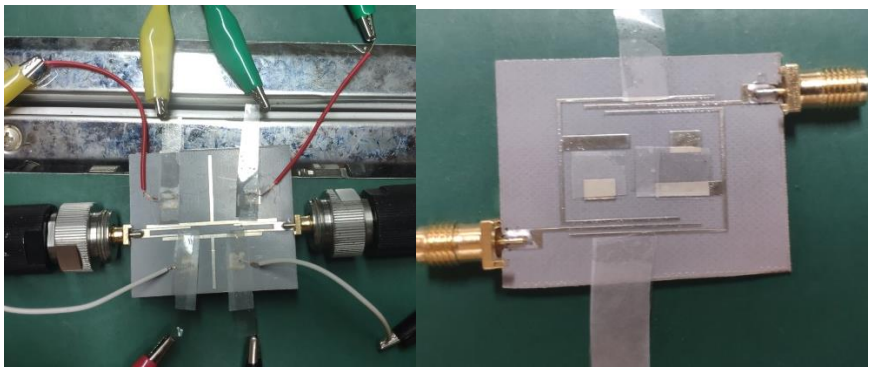

(a) (b)

 doi:10.20944/preprints202412.1760.v1

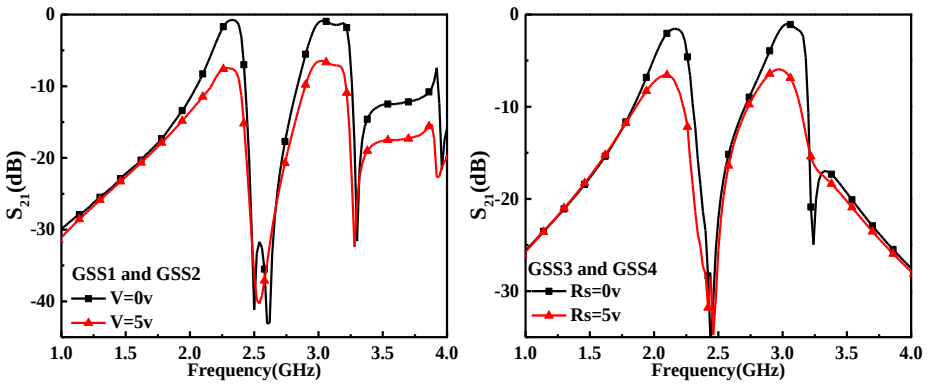

(c) (d)

Figure 5. (a)Proposed filtering dual-band filtering attenuator I. (b)Proposed filtering dual-band filtering attenuator II. (c)Measured results of dual-band filtering attenuator I. (d) Measured results of dual-band filtering attenuator II.

4. Conclusion

In this paper, a design method of tunable multifunctional attenuators by integrated GSS with microwave dual-mode resonators is proposed. Firstly, the effect of graphene on the resonant modes of common microstrip dual-mode resonators is analyzed by utilizing odd-even mode method. Then, by comparing the similarities and differences of different GSS loaded dual-mode resonators, a design method for multifunction attenuator are summarized. Finally, two kinds of multifunction attenuators using different GSS loaded dual-mode resonators are designed and fabricated according to previous analysis. The measured results show that all these multifunction attenuators can achieve controllable attenuation, which further verifies the proposed design method. Multifunctional attenuators can not only improve the integration, but also reduces the insertion loss compared with cascaded devices, which can find applications in the multifunctional RF front and the feed network of antenna array.

Author Contributions: Conceptualization, B.W.; methodology, Z.Y and Q.W.; software, Z.Y., Q.W. and C.F.; validation, Z.Y., and Q.W.; formal analysis, Q.W. and C.F.; investigation, C.F.; resources, B.W.; data curation, C.F.; writing—original draft preparation, Z.Y., Q.W. and C.F.; writing—review and editing, B.W.; visualization, Q.W.; supervision, Y.Q.; project administration, B.W.; funding acquisition, Y.Q. All authors have read and agreed to the published version of the manuscript.

Funding: This research is supported by the National Natural Science Foundation of China (NSFC) under grant number 62171348, 62201440, U19A2055, the National Key R&D Program of China (No. 2021YFA1003400), Shaanxi Science Fund for Outstanding Young Scholars under grant number 2024JC-JCQN-64, the 111 Project of China, the Fundamental Research Funds for the Central Universities.

Institutional Review Board Statement: Not applicable.

Informed Consent Statement: Not applicable.

Data Availability Statement: Not applicable.

Acknowledgments: Not applicable.

Conflicts of Interest: The authors declare no conflict of interest.

References

1. M. Bozzi, L. Pierantoni, and S. Bellucci, “Applications of graphene at microwave frequencies,” Radioengineering, vol. 24, no. 3, pp. 661–669, Sep. 2015.
2. M. Dragoman et al., “Graphene for Microwaves,” IEEE Microw. Mag., vol. 11, no. 7, pp. 81–86, Dec. 2010.

3. L. Pierantoni, D. Mencarelli, M. Bozzi, R. Moro, and S. Bellucci "Microwave applications of graphene for tunable devices," in Proc. 9th Eur. Microw. Integr. Circuit Conf. (EuMIC), Rome, Italy, Oct. 2014, pp. 512–515.
4. L. Pierantoni, D. Mencarelli, M. Bozzi, R. Moro, and S. Bellucci, "Microwave applications of graphene for tunable devices," in 44th Eur. Microw. Conf. Oct, 2014, pp. 1456–1459.
5. S. Bellucci, M. Bozzi, A. Cataldo, R. Moro, D. Mencarelli, and L. Pierantoni, "Graphene as a tunable resistor," in Int. Semiconductor Conf. (CAS). IEEE, 2014, pp. 17–20
6. J. Chen, J. Li, and Q. H. Liu, "Designing graphene-based absorber by using HIE-FDTD method," IEEE Trans. Antennas Propag., vol. 65, no. 4, pp. 1896–1902, Apr. 2017.
7. D. Yi, X. Wei, and Y. Xu, "Transparent microwave absorber based on patterned graphene: design, measurement, and enhancement," IEEE Trans. Nanotechnol., vol. 16, no. 3, pp. 484–490, May 2017.
8. D. Yi, X. Wei, and Y. Xu, "Tunable microwave absorber based on patterned graphene," IEEE Trans. Microw. Theory Tech., vol. 65, no. 8, pp. 2819–2826, Aug. 2017.
9. B Wu, Y.H. Zhang, Y.T. Zhao, et al., "Compact nine-way power divider with omnidirectional resistor based on graphene flake," IEEE Microw. Wireless Compon. Lett., vol. 28, no.9, Sep. 2018.
10. J.J. Zhang, B. Wu, et al., "Two-dimensional Highly Sensitive Wireless Displacement Sensor with Bilayer Graphene-based Frequency Selective Surface," IEEE Sensors Journal, 2021,21(21), 23889-23897.
11. H.R. Zu, B.Wu, et al., "Circularly Polarized Wearable Antenna with Low-Profile and Low Specific Absorption Rate Using Highly Conductive Graphene Film," IEEE Antennas Wireless Propag. Lett. 2020,19(12), 2354-2358.
12. L. Pierantoni et al., "Broadband microwave attenuator based on few layer Graphene flakes," IEEE Trans. Microw. Theory Techn., vol. 63, no. 8, pp. 2491–2497, Aug. 2015.
13. B Wu, Y.H. Zhang, Haoran Zu, Chi Fan, and Weibing Lu, "Tunable Grounded Coplanar Waveguide Attenuator Based on Graphene Nanoplates," IEEE Microw. Wireless Compon. Lett. vol. 29, no. 5, pp. 330–332, May. 2019.
14. M. Yasir, P .Savi, S. Bistarelli, et al., "A planar antenna with voltage-controlled frequency tuning based on few-layer graphene," IEEE Antennas Wireless Propag. Lett., vol. 16, pp. 2380–2383, 2017.
15. M. Yasir, S. Bistarelli, A. Cataldo, M. Bozzi, L. Perregrini, and S. Bellucci, "Tunable phase shifter based on few-layer graphene flakes," IEEE Microw. Wireless Compon. Lett., vol. 29, no. 1, pp. 47–49, Apr. 2019.
16. C.Fan, B.Wu, et al.,"Millimeter-wave Pattern Reconfigurable Vivaldi Antenna Using Tunable Resistor Based on Graphene," IEEE Trans. Antennas and Propagation, 2020,68(6),4939-4943.
17. A.-Q. Zhang, W.-B. Lu, Z.-G. Liu, H. Chen, and B.-H. Huang, "Dynamically tunable substrate-integrated-waveguide attenuator using graphene," IEEE Trans. Microw. Theory Techn., vol. 66, no. 6, pp. 3081–3089, Jun. 2018.
18. A.-Q. Zhang, W.-B. Lu, Z.-G. Liu, H. Chen, "Dynamically tunable attenuator on a graphene-based microstrip line," IEEE Trans. Microw. Theory Techn., vol. 67, no. 2, pp. 746–753, Feb. 2019.
19. A.-Q. Zhang, W.-B. Lu, Z.-G. Liu, H. Chen, "Graphene-based dynamically tunable attenuator on a coplanar waveguide or a slotline," IEEE Trans. Microw. Theory Techn., vol. 67, no. 1, pp. 70–77, Jan. 2019.